

DESIGN AND ANALYSIS OF BIDIRECTIONAL BUCK-BOOST CONVERTER FOR GRID TO PHEV AND PHEV TO HOME

Sharmila D¹, P. Maruthupandi²

Department of Electrical and Electronics Engineering, Government College of Technology, Anna University, Coimbatore-641013, India

E-mail: Shar71772173204@gct.ac.in¹, pandi@gct.ac.in²

Abstract

Nowadays, the use of Electric Vehicles (EV) is rapidly increasing. The batteries of the EV are charged when its demand is low, and the energy would then be stored to act as a kind of reserve that could be used when necessary. A new design of “bidirectional DC-DC buck boost converter” is suggested for transferring electrical power between the grid and an electric vehicle, as well as between an electric vehicle and the residence. While using grid energy to charge the car battery, the Grid to Vehicle (G2V) mode utilizes a buck mode DC-DC converter operation. The Vehicle to Home (V2H) function uses the battery's stored energy to power dwellings off the grid when the DC-DC converter is running in boost mode. The battery's Status of Charge is determined using an enhanced Kalman filter. Proportional-integral controllers are used in bidirectional buck boost converters to maintain a consistent voltage on both the high voltage and low voltage sides. Phase angle control is used for G2V and V2H operations on the H-Bridge inverter that the DC-DC converter is coupled with. The proposed circuit is simulated in MATLAB, and the results are reviewed.

Index Terms – Bidirectional buck-boost converter, G2V, V2G, Status of Charge (SOC)

1. Introduction

The use of variable renewable energy and widespread electrification of vehicles are being encouraged by laws around the world that are aimed at reducing carbon emissions. The idea of utilising electric vehicles' large energy storage capacity as an energy source has been proposed in this work. The battery of Electric Vehicle (EV) should ideally be charged at times

of low demand and the stored energy should be accessible for use by households [2]. The converter functions in both directions and becomes an interface between the grid and the battery pack. Bidirectional buck-boost converters enable Grid to Vehicle (G2V) and Vehicle to Home (V2H) operation modes with high quality performance [2]. The low voltage level of the EV is made stable employing a DC-DC converter that operates in bidirectional mode, and this compensates the mismatch in the line voltage and the battery voltage [2].

A high voltage gain ratio over a wide range can be achieved by adjusting turns-ratio of the inductively coupled converter [4]. The bidirectional converter is used in G2V and V2H applications for step-up and step-down operations. This converter has a straightforward structure in addition to a wide range of high voltage gain, low P stress on semiconductor components [4]. Low rated power switches may be used in the bidirectional DC-DC buck-boost converter to increase efficiency. A Proportional-Integral (PI) controller is used to keep the voltage constant on both the High-Voltage (HV) and Low-Voltage (LV) sides of the bidirectional buck boost converter. Estimating the State of Charge (SOC) of the battery is one of the biggest challenges [10]. To ensure effective energy management and avoid overcharging or undercharging the battery, a good SOC estimation is necessary [10]. SOC cannot be measured directly; hence it must be estimated accurately using indirect methods [1]. Real-time SOC is achieved via a method known as an EK filter, because the battery model utilised is nonlinear.

2. Existing Circuit

The DC-DC converter consists of Switches S1, S2, Q1, Q2, capacitor C1 and C2 as shown in fig.1. Inductor L1 and L2 are also a part of it [2]. A lithium-ion battery is coupled with an extensible, non-isolated bidirectional DC-DC. This converter is extensible, has a straightforward structure, and is simple to operate switches S1, S2, Q1, Q2. Each state consists of two alternative power switches. The application of n stages, also increases the VTR for both directions. Fig.2 shows a bidirectional DC-DC buck boost converter and a bidirectional AC-DC [2].

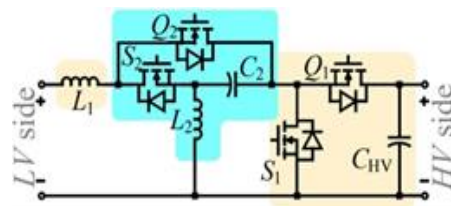


Figure 1. Non-isolated extendable bidirectional DC-DC converter

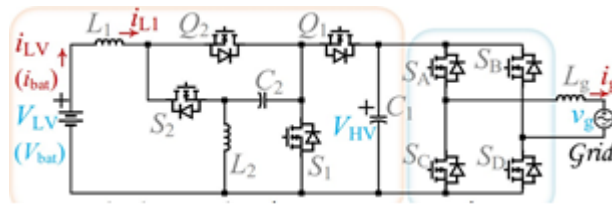


Figure 2. Existing Circuit

3. Proposed Block Diagram

A bi-directional AC-DC converter that converts AC to DC and DC to AC supply is what the proposed system is made up of. As seen in Fig.3, the proposed bi-directional DC-DC buck boost converter is used to send electricity from the grid to homes and from electric vehicles to residences. To maintain a consistent voltage on the converter's high voltage and low voltage sides, a proportional-integral controller is employed. The H-Bridge inverter is built within the DC-DC converter and used for both Grid to Vehicle (G2V) and Vehicle to Home (V2H) operations. The battery stores the energy that is provided to the vehicle by the grid. When there is no grid supply, the battery's energy is used to power home loads. Using an extended Kalman filter, the SOC of the battery is estimated.

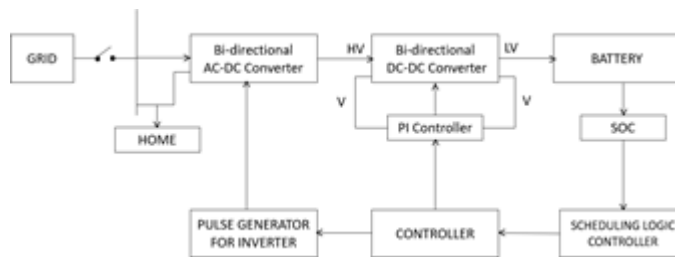


Figure 3. Proposed Block Diagram

4. Proposed Circuit

The suggested DC-DC converter is composed of five switches (S1, S2, Q1, Q2, and Q3), four capacitors (C1, C2, Co(1, 2)), and two inductors (L1 and L2). Throughout the whole switching period (Ts), the switches and body diodes conduct alternately. A conventional single-phase full-bridge DC-AC converter is utilised with unipolar PWM modulation to connect the bidirectional DC-DC converter to the AC grid as shown in fig. 4.

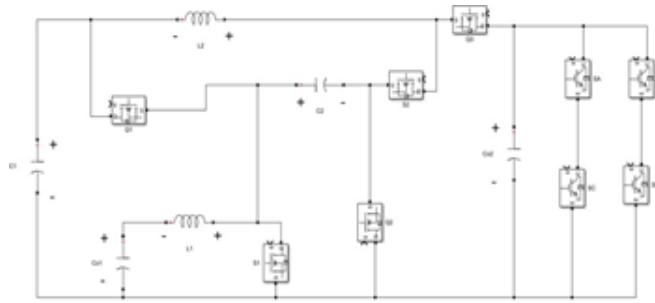


Figure 4. Proposed circuit diagram

5. Modes of Operation

A. Step-down Mode

The VHV and VLV sides are connected in turn to a DC supply and the load. The following are the two states for CCM operation (four states for DCM):

State 1 CCM $[0 - t_1]$: Q1, Q2, and Q3 are on throughout this period, but S1 and S2 are off, as seen in Fig. 5(a). During this time, the input DC supply and energy released from C1, charge L2. As a result, L2's current increases, while C2's energy increases L1's energy.

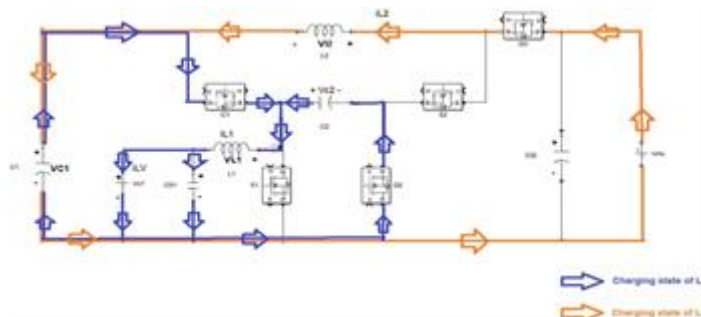


Figure 5(a). State 1 CCM $[0-t_1]$

State 2 CCM $[t_1 - T_s]$: Q1, Q2, and Q3 are on throughout this period, but S1 and S2 are off, as seen in Fig. 5(b). The input DC supply and the power that C1 charge, releases L2. As a result, L2's current increases, while C2's energy increases L1's energy.

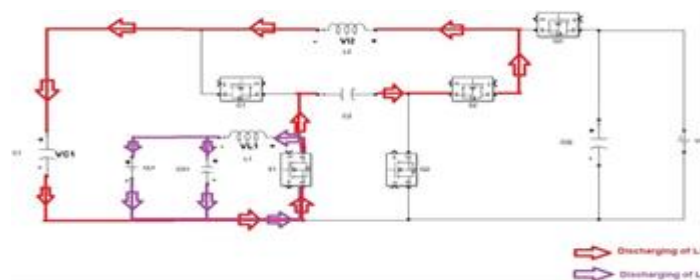


Figure 5(b). State 2 CCM [t1-Ts]

B. Step-up Mode

Power travels from the VLV side to the VHV side in this mode. The following are the 2 states for CCM operation (4 states for DCM):

State 1 CCM: S1 and S2 are both on throughout this period, in accordance with Fig. 5(c), but Q1, Q2, and Q3 are off. L1 is charged by the input DC source in this state. As a result, the current through L2 grows while L2's energy from C1 and C2 increases.

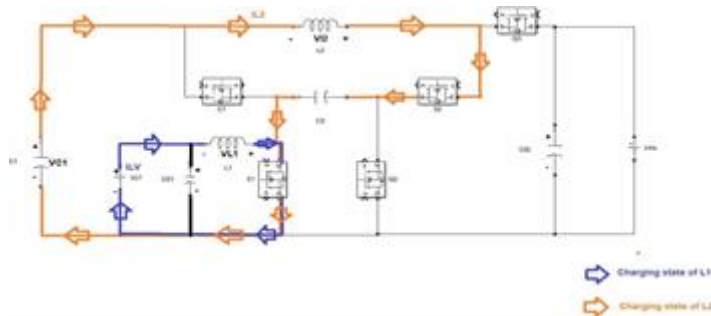


Figure 5(c). State 1 CCM (Step-up Mode)

State 2 CCM [t1 – Ts]: In contrast to state 1, S1 and S2 are switched off while Q1, Q2, & Q3's body diodes are conducting as depicted in Fig. 5(d). The capacitors C2 receive the energy that the inductor L1 releases. Similar to L2, the VHV side receives the energy emitted by L2. The power switches remain off. Inductors reach zero current flow. A full period Ts is spent at the conclusion of this interval. When taking into account these intervals, the duty cycles D1 and D2 can be regarded as the points at which the current through L1 and L2 ceases to flow, respectively.

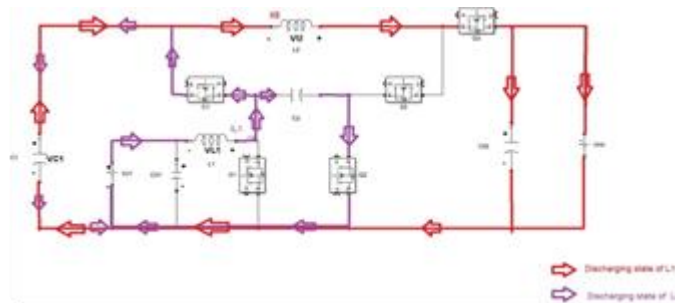


Figure 5(d). State 2 CCM (Step-up Mode)

6. Steady State Calculation

The development of mathematical equations that characterise the switching functions of the buck converter and boost converter with CCM and DCM mode is used to calculate steady states.

A. STEP-UP MODE

State 1 and 2 are the next states in step-up mode. From 0 to t_1 in state 1, the conduction mode is discontinuous. In state 2, the continuous conduction mode runs from time t_1 to time t_s , and the discontinuous conduction mode runs from time t_1 to time t_2 .

State 1: CCM & DCM [0- t_1]

$$V_{L1} = L1 \cdot di_{L1}/dt = V_{LV}$$

$$V_{L2} = L2 \cdot di_{L2}/dt = V_{C1} + v_{c2}$$

State 2: CCM (t_1 - T_s) & DCM [t_1 - t_2]

$$v_{L1} = V_{LV} - v_{c2} \quad v_{L2} = -V_{HV} + v_{c2}$$

The voltage across C1 and C2 are equal,

$$v_{c1} = v_{c2}$$

Applying volt-second balance on L1 & L2,

$$D(V_{LV}) + (1-D)(V_{LV} - V_{C1}) = 0 \quad (1)$$

$$D(V_{C1} + V_{C2}) + (1-D)(-V_{HV} + V_{C1}) = 0$$

Voltage across C1 and C2 can be determined by,

$$V_{C1} = V_{C2} = V_{LV}/(1-D) \quad (2)$$

Gain for step up mode is obtained by,

$$M_{\text{step-up(CCM)}} = V_{HV}/V_{LV} = 1 + D/(1-D)^2 \quad (3)$$

B. STEP-DOWN MODE

From 0 to t_1 in state 1, the conduction mode is discontinuous. In state 2, the continuous conduction mode runs from time t_1 to time t_s , and the discontinuous conduction mode runs from time t_1 to time t_2 .

State 1: CCM and DCM [0- t_1]

$$V_{L1} = L_1 \frac{di_{L1}}{dt} = -V_{LV} + V_{C2}$$

$$V_{L2} = L_2 \frac{di_{L2}}{dt} = V_{HV} - V_{C2}$$

State 2: CCM ($t_1 - T_s$) and DCM [$t_1 - t_2$]

$$V_{L1} = L_1 \frac{di_{L1}}{dt} = -V_{LV}$$

$$V_{L2} = L_2 \frac{di_{L2}}{dt} = -V_{C1} - V_{C2}$$

Volt-second balance on L1 and L2 is applied.

$$D(-V_{LV} + V_{C1}) + (1-D)(-V_{LV}) = 0$$

$$D(V_{HV} - V_{C1}) + (1-D)(-V_{C1} - V_{C1}) = 0$$

Average Voltage across C1 and C2 can be determined by,

$$V_{C1} = V_{C2} = V_{LV} / D \quad (4)$$

Gain for step down mode is obtained by,

$$M_{\text{step-down(CCM)}} = V_{LV} / V_{HV} = D^2 / (2-D) \quad (5)$$

7. Design Consideration

Duty cycle calculation

The actual duty cycle is crucial because, if it is slightly increased from the theoretical ideal efficiency value, the operating peak current and the accompanying magnetic fields may be increased significantly. Current ripple of inductor L1 & L2 for step down are obtained in eq.(6) and (7) & for step up, it is obtained in eq.(8) and (9).

Step-down:

$$\Delta i_{L1} = (1-D) / (L_1 f_s) * V_{LV} \quad (6)$$

$$\Delta i_{L2} = 2(1-D) / (L_2 f_s D) * V_{LV} \quad (7)$$

Step- up:

$$\Delta i_{L1} = D / (L_1 f_s) * V_{LV} \quad (8)$$

$$\Delta i_{L2} = 2D / (L_2 f_s (1-D)) * V_{LV} \quad (9)$$

Passive component design

Critical values of inductor L1 and L2 are calculated, also the critical values of capacitor C1, C2, C01 and C02 are calculated.

Step-down:

$$L1 \geq 1-D / \Delta i L1 f_s * VLV$$

$$L2 \geq 2(1-D) / \Delta i L2 f_s D * VLV$$

Step- up:

$$L1 \geq D VLV / \Delta i L1 f_s$$

$$L2 \geq 2D VLV / \Delta i L2 f_s (1 - D)$$

Step-down:

$$L1 \geq (1-D) VLV / 2ILVf_s, L2 \geq (2-D) (1-D) / (D2 ILVf_s) * VLV$$

Step-up:

$$L1 \geq D VLV / 2ILVf_s$$

$$L2 \geq (D) (1+D) / (1-D2) ILVf_s * VLV$$

The values of C1, C2 and C0(1,2) can be obtained in eq.(10) and (11).

Step-down:

$$C1,2 \geq D(1-D) ILV / \Delta VC1,2 f_s (2 - D) \quad (10)$$

$$C01 \geq (1-D) VLV / 8\Delta VC01(f_s)L1$$

Step-up:

$$C1,2 \geq D(1-D) ILV / \Delta VC1,2 f_s (1 + D) \quad (11)$$

$$C02 \geq D(1-D)^2 VLV / \Delta VC02 f_s (1 + D)$$

8. State of Charge Estimation

The algorithm shown in fig.6, is applied to nonlinear system

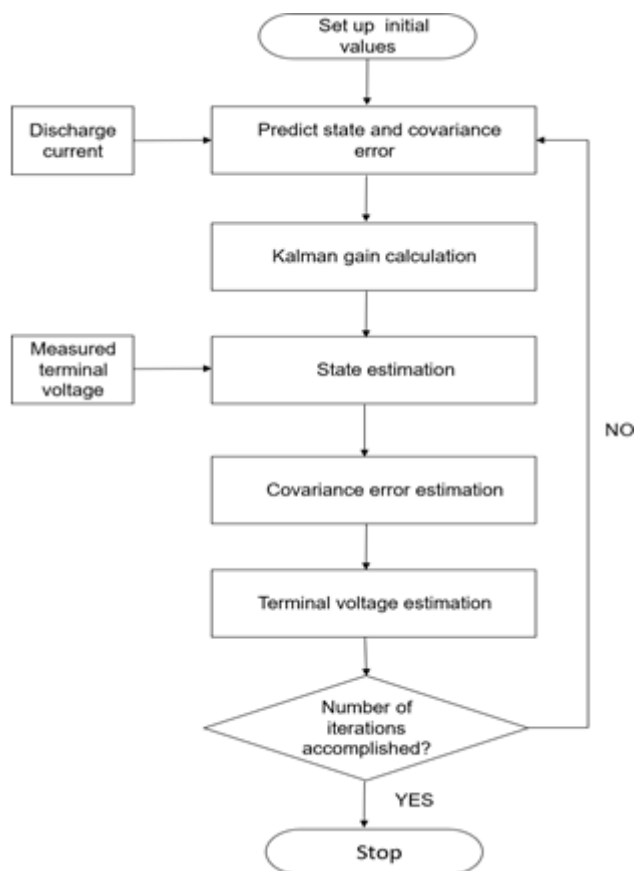


Figure 6. Flow chart of algorithm

$$V_2 = -1/R_1 * C_2 (V_2 - V_1)$$

$$V_{out} = V_{oc} - R_s * i(t)$$

R1 parameters are calculated by,

$$R_1 = -0.0341 * i(t)^3 + 3.419 * i(t)^2 - 93.9 * i(t) + f$$

$$V_1 = 1/R_1 * C_1 (V_2 - V_1) - 1/C_1 i(t)$$

The system i/p is defined as $u(t) = i(t)$ and the o/p as

$$y(t) = V_{out}.$$

W and V represent the process noise and measurement noise, respectively [1].

$$x = f(x, u) + w$$

$$y = g(x, u) + v \quad (23)$$

$$f(x, u) = -u C_1 + 1 (R_1 * C_1 (V_2 - V_1) - 1 (R_1 * C_1 (V_2 - V_1)$$

$$g(x, u) = V_{oc} - R_s * u$$

Each is regarded as white Gaussian noise. Battery model linearization comes next. First order Taylor series are used to expand the functions $f(x, u)$ and $g(x, u)$, respectively [1].

The following equations set represents the linearised model.

$$\dot{x} = A * x + B * u + w \quad (12)$$

$$y = C * x + D * u + v$$

The nonlinear equations of the model were therefore used to create a state space formulation for use with the EKF [1]. It was also discovered that employing this estimation technique produced fewer mistakes than did relying just on the battery model.

9. Simulations and Results

OVERALL SIMULATION (G2V) AND (V2H)

Overall simulation of G2V AND V2H shown in fig.7, consists of both the bidirectional converter (DC-DC and the AC-DC). In G2V mode, the bidirectional AC-DC converter converts the AC supply to DC supply. The H bridge inverter is implemented with phase angle control method. The high voltage from grid is converted to low voltage with buck converter and low voltage is stored in the battery and the battery gets charged. In V2H, the low voltage from battery is boosted to high voltage and the battery starts to discharge to supply the home loads. To calculate SOC of the battery, an EKF battery state of charge estimation is implemented. The G2V and V2H is simulated in MATLAB and the results are analysed.

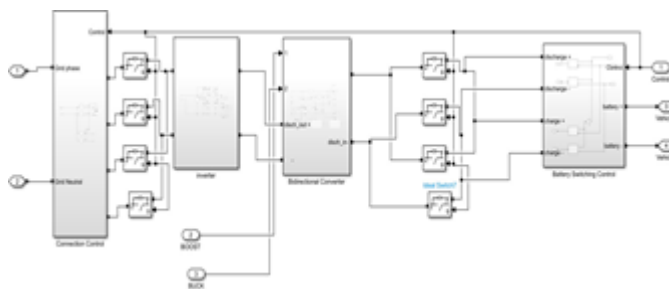


Figure 7. Overall simulation of grid to vehicle and vehicle to home

Table 1. Simulation Parameters

PARAMETERS	VALUES
Grid voltage (V_g)	230V
Battery voltage (V_b)	72V
Battery capacity (Ah)	30

Switching frequency (fs)	50 Hz
Inductors L1, L2	0.4mH & 1mH
Capacitor C1, C2, C01, C02	22 μ F, 22 μ F & 680 μ F

Grid to Vehicle Simulation

G2V mode is represented in fig.8. The bidirectional AC-DC converter converts AC supply to DC supply. The H bridge inverter is implemented with phase angle control method. The high voltage from grid is converted to low voltage with buck converter and low voltage is stored in the battery and the battery gets charged.

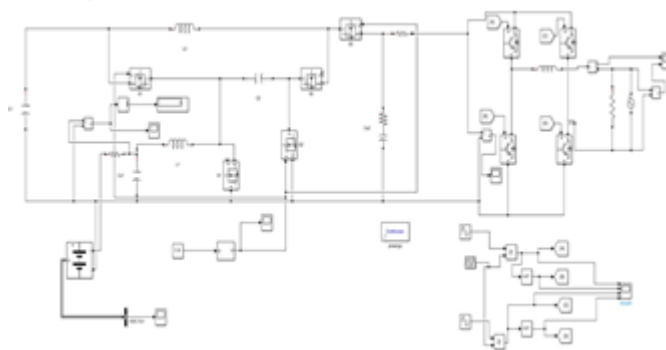


Figure 8. G2V simulation

A. Switching pulse of converter in buck mode

Gating signal is given to switches Q1, Q2 and Q3, where the PWM generator generates the pulse. Q1, Q2 and Q3 are turned “ON” in DC-DC converter for Grid to Vehicle mode. Pulse is obtained is from 0 to 1. When the switch is “ON”, conduction of pulse is at 1, and when the switch is “OFF, the pulse is at 0 and no conduction occurs. In fig.9, the pulse waveform is displayed. Time is shown by the X axis & pulse's amplitude is represented by the Y axis.

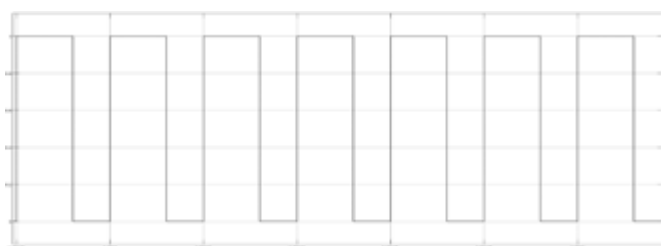


Figure 9. Output of switching pulse of converter in buck mode

B. Switching pulse of Inverter in buck mode

Here, the carrier signal and the two reference signals are compared & for Grid to Vehicle the phase angle control method is used for rectification operation. In H bridge inverter, when switches A and C are “ON”, the pulse is at 1, and when the inverter switches B and D are “OFF”, the pulse is at 0. Fig.10 illustrates the switching pulses of the inverter output waveform that were acquired. Time is represented by X axis, and pulse amplitude is shown in the Y axis.

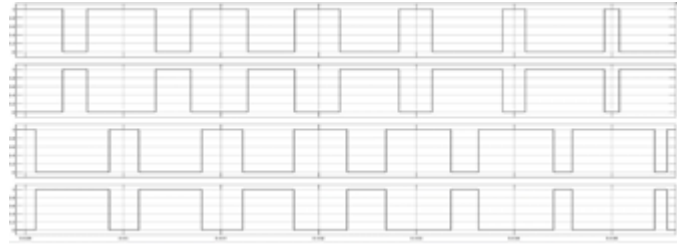


Figure 10. Output of Switching pulse of inverter in buck mode

C. Grid current and voltage

In grid side, current and voltage waveforms are obtained with peak amplitude of 325V and peak current 80A. Grid current and voltage are in out of phase. Fig.11 depicts the output waveforms acquired. Y axis represents magnitude of current and voltage, and X axis represents the time.

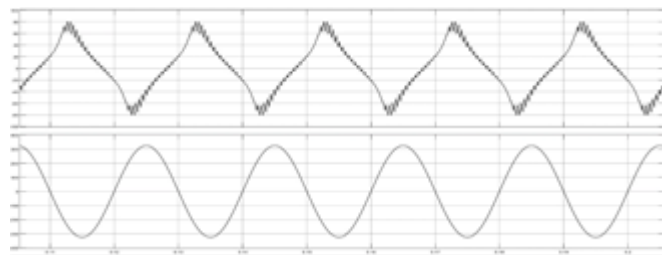


Figure 11. Output grid current and voltage

D. Battery charging

From the grid supply, the battery is charged, where the initial state of charge is 20%. The battery gets charged from 20%. Battery charging output waveform is shown in fig.12. The time and the state of charge are shown in X and Y axes respectively.

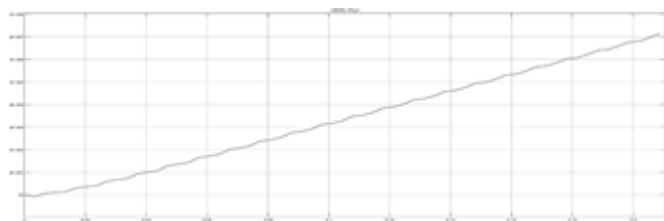


Figure 12. Output of battery charging

Vehicle to Home Simulation

In V2H, the low voltage from battery is boosted to high voltage and the battery starts to discharge to supply the home loads. To calculate the SOC of the battery an EKF battery state of charge estimation is implemented. The H bridge inverter is implemented with phase angle control method. Vehicle to home mode is simulated in Matlab and is shown in fig.13.

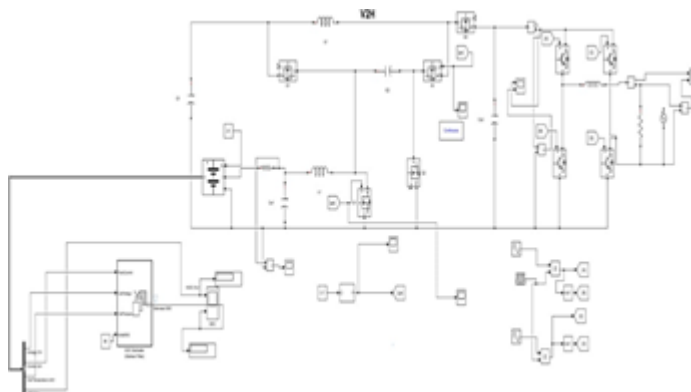


Figure 13. V2H simulation

A. Switching pulse of converter in boost mode

Gating signal is given to S1 & S2. Q1, Q2 & Q3 are turned off, where the PWM generator generates the pulse. S1 & S2 are turned “ON” in DC-DC converter for Vehicle to Home mode. Pulse is obtained from 0 to 1. When the switch is “ON”, conduction of pulse is at 1, and when the switch is “OFF”, the pulse is at 0 and no conduction occurs. The pulse waveform is shown in fig.14.

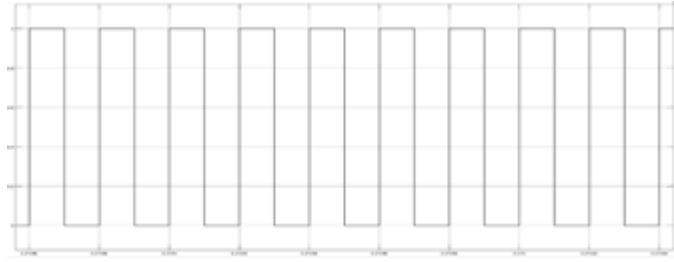


Figure 14. Output switching pulse of converter in boost mode

B. Switching pulse of inverter in boost mode

The two reference signals are compared with carrier signal and for vehicle to grid, the phase angle control method is used for DC-AC operation. The time and the pulse amplitude are shown in X and Y axes respectively.

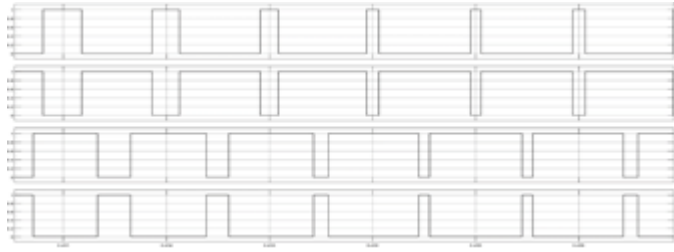


Figure 15. Output of Switching pulse of Inverter in boost mode

C. Load current and voltage

Load current and voltage output waveform are obtained and shown in fig.16. Y axis represents magnitude of current and voltage respectively and X axis represents time.

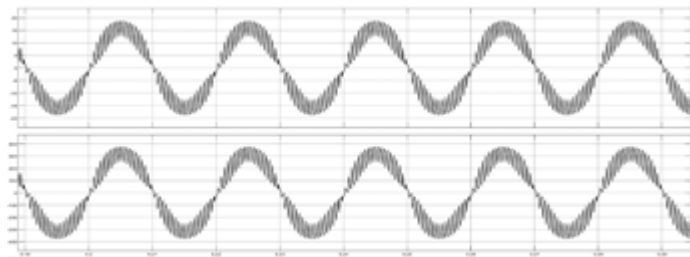


Figure 16. Output load current and voltage

D. Battery Discharge

Energy stored in the battery is discharged. It starts discharging from initial SOC i.e., 80%. Battery discharging output waveform is obtained and shown in fig.17.

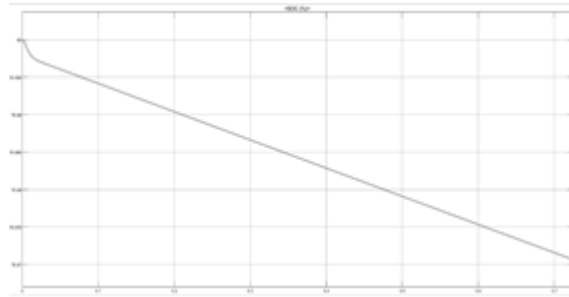


Figure 17. Output of battery discharging

G2v with SOC Estimator

To calculate the SOC of the battery, an EKF method is implemented in Matlab. The Kalman filter linearizes about an estimate of the current mean and covariance. The G2V is shown in fig.18. Bidirectional AC-DC converter converts the AC supply to DC supply. The H bridge inverter is implemented with phase angle control method.

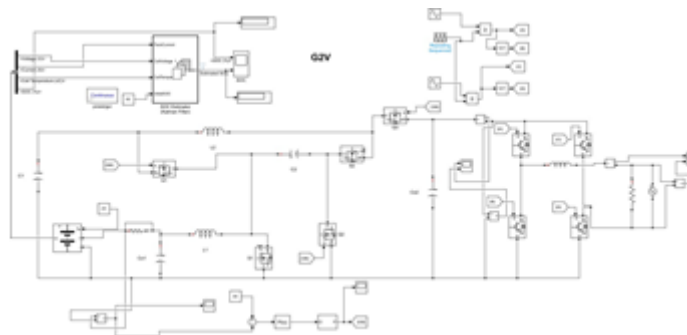


Figure 18. G2V with SOC estimator simulation

Output waveform

During battery charging mode, the actual SOC is 60 and the estimated SOC is 70. Estimated battery SOC is increased gradually and stepped waveform is obtained and shown in fig.19.

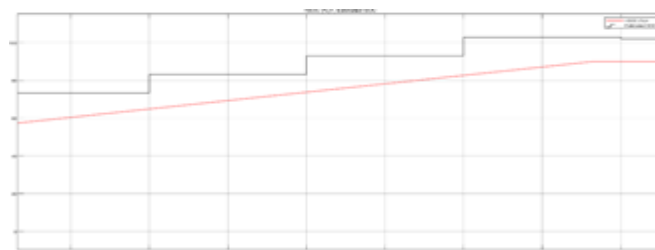


Figure 19. Output of SOC estimation for G2V

V2H WITH SOC ESTIMATOR

An EKF approach is constructed in Matlab to calculate the battery's SOC. A Kalman filter linearizes about a current mean and covariance estimate. In V2H mode, the battery's low voltage is increased to a high voltage and the battery begins to discharge in order to power the home's loads. An EKF battery state of charge estimation is used to calculate the SOC of the battery. Phase angle control approach is used to create the H bridge inverter. Matlab simulates the vehicle to home mode, which is displayed in fig.20.

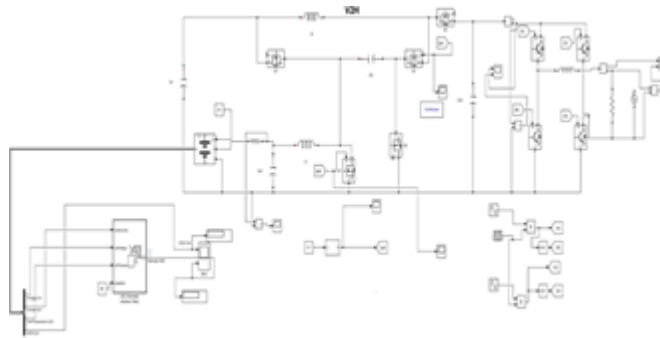


Figure 20. V2H with SOC estimator simulation

Output waveform

During battery charging mode, the actual SOC is 60 and the estimated SOC is 59. Estimated SOC stepped waveform, gradual battery discharge and stepped waveform are obtained and shown in fig.21.

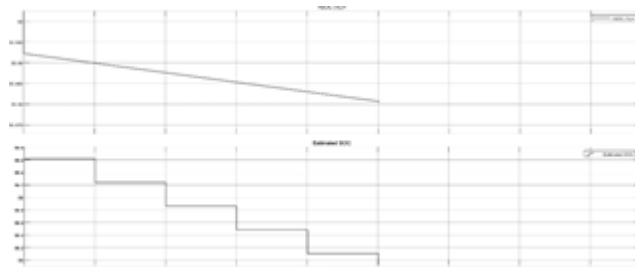


Figure 21. Output waveform of V2H with SOC estimator

10. Conclusion

The design of Grid to PHEV and the PHEV to home requires enhanced bidirectional DC-DC and AC-DC converters with high voltage gain. This converter features common ground, low-rated switches, extendibility, voltage gains (step-up and step-down), and the capacity to function in both directions. To estimate the cell SOC, an enhanced Kalman filter method is used. Consequently, a state space formulation for an extended Kalman filter is constructed from the nonlinear equations defining the model. In order to maintain a consistent voltage on both HV & LV sides, bidirectional buck boost converters use PI controllers. The suggested circuit results are observed using the MATLAB.

References

- [1] Sonia Carina Lopes da, Costa, Armando Sousa Araujo and Adriano da Silva Carvalho, “Battery State of Charge Estimation Using Extended Kalman Filter”, *IEEE Trans. Ind Electron.*, vol.6, no.2, pp.22-24, June 2016.
- [2] Seyed hossein hosseini, Reza Ghazi, Hamed Heydari-doostabad, “An Extendable Quadratic Bidirectional DC-DC Converter for V2G and G2V Applications”, year of publication-2021. *IEEE Transactions on Industrial Electronics*, 68 (6): 4859-4869.
- [3] Arun Kumar Verma and Bhim Singh, “Grid to Vehicle and Vehicle to Grid Energy Transfer using Single-Phase Bidirectional AC-DC Converter and Bidirectional DC-DC converter”, *IEEE Trans. Ind Electron.*, vol.2, pp.936-942, 09 February 2012.
- [4] Y.-P. Hsieh, J.F. Chen, L.S. Yang, C.-Y. Wu, and W.-S. Liu, “High Conversion- Ratio Bidirectional DC–DC Converter with Coupled Inductor”, *IEEE Trans. Ind. Electron.*, vol. 61, no. 1, pp. 210–222, Jan. 2014.
- [5] M. J. E. Alam, K. M. Muttaqi, and D. Sutanto, “Effective Utilization of Available PEV Battery Capacity for Mitigation of Solar PV Impact and Grid Support With Integrated V2G Functionality”, *IEEE Trans. Smart Grid*, vol. 7, no. 3, pp. 1562– 1571, 2016.
- [6] J. Lu, Y. Wang, and X. Li, “Isolated Bidirectional DC–DC Converter with Quasi Resonant Zero-Voltage Switching for Battery Charge Equalization”, *IEEE Trans. Power Electron.*, vol. 34, no. 5, pp. 4388–4406, May 2019.

- [7] M. Eydi, S. H. Hosseini, and R. Ghazi, "A New High Gain DC-DC Boost Converter with Continuous Input and Output Currents", 2019 10th International Power Electronics, Drive Systems and Technologies Conference (PEDSTC), vol.6, no.4, pp.1394-1421, Feb 2019.
- [8] T.-F.Wu, Y.-C.Chen, J.-G.Yang, and C.-L. Kuo, "Isolated Bidirectional Full Bridge DC-DC Converter with a Flyback Snubber", IEEE Trans. Power Electron., vol. 25, no.7, pp. 1915-1922, July 2010.
- [9] H. Jeong, M. Kwon, and S. Choi, "Analysis, Design, and Implementation of a High Gain Soft-Switching Bidirectional DC-DC Converter with PPS Control", IEEE Trans. Power Electron., vol. 33, no. 6, pp. 4807-4816, June 2018.
- [10] M. Iwan Wahyuddin, Purnomo Sidi Priambodo, Harry Sudiby, "State of Charge (SoC) Analysis and Modeling Battery Discharging Parameters", IEEE Trans., vol.23, no 6, pp.1915-1922, May 2018.